Reducing Model Uncertainty Effects in Flexible Manipulators Through the Addition of Passive Damping

T.E. Alberts
Old Dominion University
Norfolk, VA 23508

1. Abstract

An important issue in the control of practical systems is the effect of model uncertainty on closed loop performance. This is of particular concern when flexible structures are to be controlled, due to the fact that states associated with higher frequency vibration modes are truncated in order to make the control problem tractable. In this paper we employ digital simulations of a single-link manipulator system to demonstrate that passive damping added to the flexible member reduces adverse effects associated with model uncertainty. A controller was designed based on a model including only one flexible mode. This controller was applied to larger order systems to evaluate the effects of modal truncation. Simulations using an LQR design assuming full state feedback illustrate the effect of control spillover. Simulations of a system using output feedback illustrate the destabilizing effect of observation spillover. The simulations reveal that the system with passive damping is less susceptible to these effects than the untreated case.

2. Introduction

Many in-space robotic operations will require arms capable of very long reach, while like other space structures, they must be lightweight. Because such arms are likely to be highly compliant (as is the space shuttle RMS arm), control strategies designed to accommodate structural flexibility must be considered. Controlling flexible structures through purely active measures can be cumbersome in terms of hardware and computation time requirements. Moreover, active controllers for flexible structures are subject to instability and other problems associated with model uncertainty. The burden of active control can be reduced by augmenting active control with passive damping. This enhances system stability and reduces the adverse affects of model uncertainty, thereby providing justification for the use of low order dynamic models and controllers.

In this paper we consider a single-link, single-axis arm which rotates in the horizontal plane about a pinned hub in response to a control torque $\tau(t)$. The system, illustrated in Figure 1, and the models employed in this investigation are based upon a laboratory version of the arm that has been used in experimental investigations [1-4] at Georgia Tech. The flexible member is a long slender beam that is assumed infinitely stiff in vertical bending but flexible in horizontal bending.

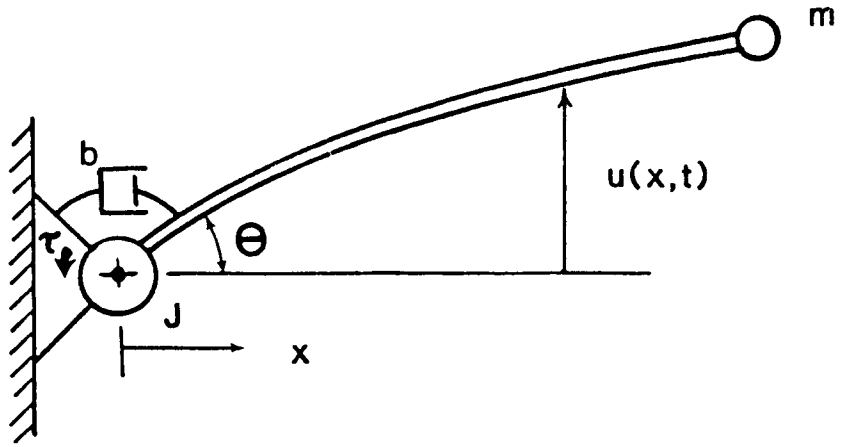

Figure 1. System Configuration

The pinned hub has rotary inertia J. A point payload mass m is fixed to the beam's tip. Although, manipulators sometimes carry payloads that have significant rotary inertia, the effect of this inertia is qualitatively similar to that of a point mass for the configuration considered, and hence payload inertia is not included here. Friction in the pinned joint is represented by a rotary viscous dashpot. This configuration is viewed as being representative of lightweight, large payload capacity manipulators. Parameters and dimensions for the arm that the system considered in this paper are tabulated in Appendix A.

Damping augmentation is provided by a constrained viscoelastic layer damping treatment [2,5]. The approach involves bonding a thin film of viscoelastic material to the flexible member's surface. This viscoelastic layer in turn has a stiff elastic constraining layer bonded to its surface. The combined system forms a sandwich-like structure illustrated in Figure 2. When elastic deflection of the structure occurs, shear induced plastic deformation is imposed in the viscoelastic layer. The energy dissipation associated with the plastic deformation provides the desired mechanical damping. The damping ratio for the untreated beam was approximately constant for all modes at .007. The treatment increased the damping ratios associated with the modes of interest (say the first six modes) by about an order of magnitude. The treated beam had a damping ratio of .03 for the first mode and the values for the 2nd through 6th modes ranged from .052 to .06. Additional damping is introduced by joint friction.

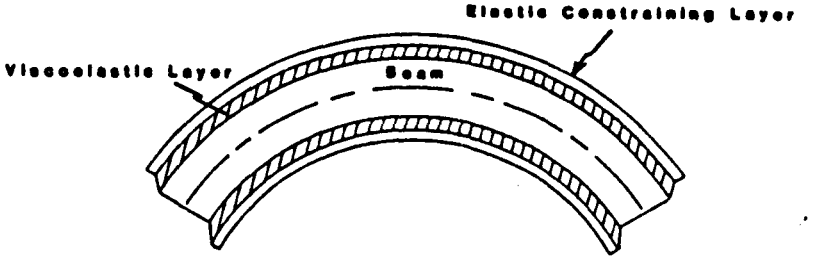

Figure 2. Treated Beam Element Under Flexure

The first step of controller design is usually the development of a "design model" that is a simplifie representation of the actual plant dynamics. The design model serves as the basis for controller design In the case of flexible mechanical systems, the design model is often a truncated representation of th actual plant, retaining only a few critical modes. This implies the assumption that a model based upon small number of vibration modes provides adequate representation of the much larger order actual plant, fo controller design purposes. The modeling error associated with the neglected modes, adversely affect closed loop system performance. In this paper, simulation results are presented to illustrate that the il effects associated with modeling error are reduced somewhat through the addition of passive damping to th system.

We consider a multivariable control system, designed according to the steady state linear quadrati regulator (LQR) approach. A four state model including only one flexible mode and the rigid body mod represents the design model. We consider the consequences of controlling larger order plants representative of the actual system, with a controller derived for the design model.

The regulator is formulated to penalize tip position and control effort. Two cases are considered The first assumes that full state feedback is available. The second case uses output feedback of ti position (v_L), tip velocity, hub angle (θ) and hub angular velocity. The controller designs are kept simpl to facilitate comparisons between the damped and undamped systems.[1]

3. Dynamic Model

Linear transfer function models for the system of interest were developed based on the assumption o small bending deflections and small hub angles. Transfer function modeling for similar systems has bee discussed by several authors [2,4,6-8] and we will not repeat the procedure here. Details on development o the model employed here may be found in [2]. The transfer function poles and zeros used in thi investigation are tabulated in Appendix B.

1/ Although it possesses some light structural damping and is affected by joint friction, we shall designate the untreated arm as "undamped".

In the interest of obtaining a state space realization from the transfer functions it is convenient to work with the partial fraction expansion form given by Equation 1. The ω's are the modal frequencies, the $\underline{\omega}$'s are the damped modal frequencies $\omega\sqrt{1-\zeta^2}$, the ζ's are modal damping ratios and n is the number of flexible modes represented. Damping due to joint friction has not been accounted for in these transfer functions but will introduced later as a form of feedback.[2] The residues λ_o and μ_o correspond to the rigid body mode.

$$G_\chi(s) = \frac{\lambda_o}{s} + \frac{\mu_o}{s^2} + \frac{\lambda_1 s + \mu_1}{s^2 + 2\zeta_1\omega_1 s + \underline{\omega}_1^2} + \cdots + \frac{\lambda_n s + \mu_n}{s^2 + 2\zeta_n\omega_n s + \underline{\omega}_n^2} \tag{1}$$

The subscript χ on $G_\chi(s)$ represents the output variable of interest. For the present study four transfer functions were required. Equation 2 summarizes these and defines the notation used here.

$$\begin{bmatrix} \text{hub angular position} \\ \text{hub angular rate} \\ \text{beam tip position} \\ \text{beam tip rate} \end{bmatrix} = \begin{bmatrix} \theta(s) \\ s\theta(s) \\ V_L(s) \\ sV_L(s) \end{bmatrix} = \begin{bmatrix} G_\theta(s) \\ G_{\dot\theta}(s) \\ G_{vL}(s) \\ G_{\dot{v}L}(s) \end{bmatrix} T(s) \tag{2}$$

Here s is the Laplace operator and T(s), $\theta(s)$ and $V_L(s)$ denote the Laplace transforms of the input torque, hub angle and tip position variables, respectively.

Figure 3 is a block diagram representation of the transfer function.

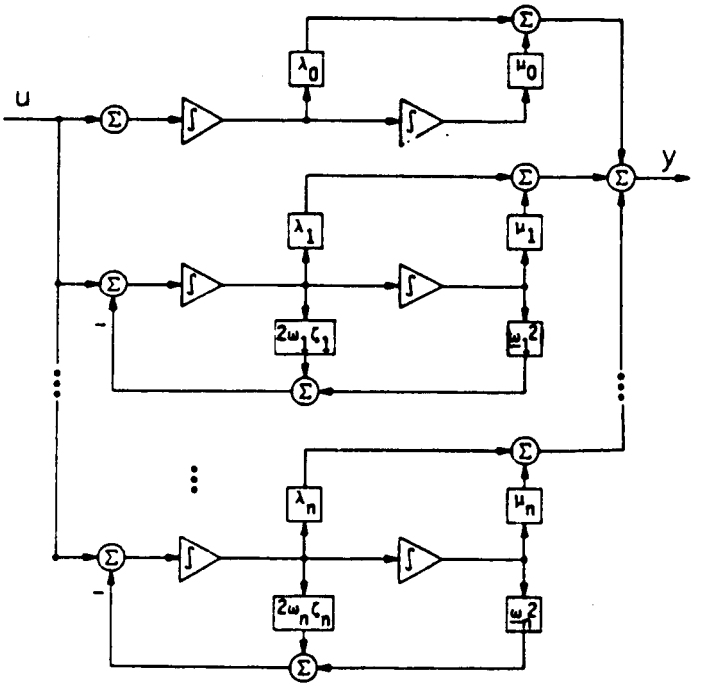

Figure 3. Block Diagram Equivalent of Equation 1

The system matrices corresponding to Figure 3 are as follows:

$$A = \begin{bmatrix} 0 & 1 & & & & \\ 0 & 0 & & & & \\ & & 0 & 1 & & \\ & & -\omega_1^2 & -2\omega_1\zeta & & \\ & & & & \ddots & \\ & & & & 0 & 1 \\ & & & & -\omega_n^2 & -2\omega_n\zeta_n \end{bmatrix}$$

$$B = [\,0\ 1\ 0\ 1\ \cdots\ 0\ 1\,]^T \qquad (3)$$

$$C_\chi = [\,\mu_0\ \lambda_0\ \mu_1\ \lambda_2\ \cdots\ \mu_n\ \lambda_n\,]$$

The leading principle 2x2 submatrix of A represents the rigid body mode in the tip and hub position transfer functions.

For each of the output variables χ there is a unique output matrix C_χ. We will denote these as C_θ, $C_{\dot\theta}$, C_{v_L} and $C_{\dot v_L}$ with the notation carrying the obvious meaning. These are assembled to form a measurement matrix representing four outputs as indicated in the measurement equation (4) given by:

$$y = \begin{bmatrix} \theta \\ \dot\theta \\ v_L \\ \dot v_L \end{bmatrix} = \begin{bmatrix} C_\theta \\ C_{\dot\theta} \\ C_{v_L} \\ C_{\dot v_L} \end{bmatrix} x = Cx \qquad (4)$$

In order to account for viscous joint damping we consider the feedback system illustrated in Figure 4.

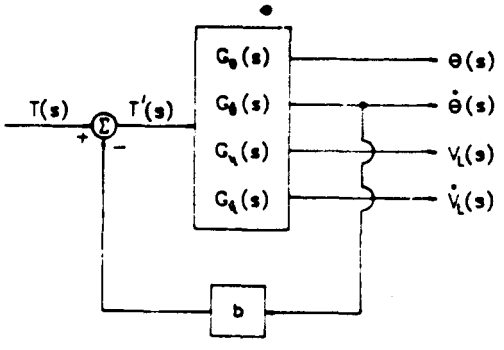

Figure 4. Block Diagram Illustrating Feedback of Joint Damping

When the effect of joint damping is introduced through boundary condition feedback, a new A matrix is formed:

$$\underline{A} = A - BC_{\dot\theta}b \qquad (5)$$

Where b is the joint damping coefficient. The analysis that follows is based upon a system model of the form $(\underline{A}, B, \underline{C})$.

4. System Representation

We wish to design a controller for a plant with 2(n+1) states, using a design model including only one vibration mode. Here n represents the number of flexible vibration modes required to provide accurate representation of the actual plant, and the additional two states represent rigid body motion. Controllers developed for the single mode system are applied to a model including three vibration modes (8 states), and one including six vibration modes (14 states). These are referred to as the plant models in the text that follows because they are intended to represent actual plants in the simulations presented here.

The system equations for the plant models are given by:

$$\dot{x}_n(t) = A_n x_n(t) + B_n u(t) \tag{6}$$
$$y(t) = C_n x_n(t)$$

Here A_n is the A matrix defined in Equation 5, in this case for an n mode approximation of the plant. Similarly the C_n matrix is the C matrix of Equation 4 for an n mode approximation.

The system equations for the design models are given by:

$$\dot{x}_1(t) = A_1 x_1(t) + B_1 u(t) \tag{7}$$
$$y(t) = C_1 x_1(t)$$

The system output vector (y) considered is of the form

$$y = [\ \theta\ \dot{\theta}\ v_L\ \dot{v}_L\ ]^T. \tag{8}$$

5. Regulator Design

The standard form of linear quadratic cost function is

$$J_c = \int_0^\infty (x^T Q x + u^T R u)\, dt \tag{9}$$

where Q is a symmetric, positive semi-definite state weighting matrix and R is a symmetric, positive definite control effort weighting matrix. Because we seek to regulate tip position, a performance index that penalizes the tip position output variable and control effort was chosen. A cost function for tip position output weighting is expressed as follows:

$$J_c = \int_0^\infty (v_L^2 + r\tau^2)\, dt \tag{10}$$

The output weighted performance index (10) is equivalent to the standard state weighted version (9) with weighting matrices given by:

$$Q = C_n^T \begin{bmatrix} 0 & & & \\ & 0 & & \\ & & 1 & \\ & & & 0 \end{bmatrix} C_n \quad , \qquad R = [r] \tag{11}$$

The system (A_n, B_n, C_n) represents an actual plant with dynamics that are either incompletely known or too cumbersome to permit the use of the full model in controller design. The four state design model (A_1, B_1, C_1) will serve as an approximation to the actual plant for controller design purposes. In this case C_1 replaces C_n in the state weighting matrix Q (11)

Two attractive features of the tip position weighted cost function (10) are that it has only one parameter (r) to vary, and that a given value of r can be expected to impose similar performance demands on both systems (damped and undamped). Reducing the value of r decreases the penalty on control effort and is therefore equivalent to demanding higher performance at the expense of increased control energy.

6. State Feedback

In a system with decoupled modes, such as the Jordan canonical realization of Equation 3, a state feedback law

$$u = -K_1 x_1 \tag{12}$$

designed to stabilize the reduced order system (7) will stabilize the actual system (6), provided that the truncated modes are asymptotically stable. The neglected modes can, however, be excited at their natural frequencies in response to the applied control input. This effect is called control spillover [9,10] in the literature related to controlling flexible spacecraft. The system we are considering has a small amount of modal coupling, due to the introduction of viscous joint damping using Equation 5. Since we normally do not

expect viscous damping to destabilize a system, it is reasonable to expect that the state feedback law (12) will stabilize the plant models of interest.

In this section we design a controller based on the output weighted performance index (10). We assume that the first four elements of the state vector are somehow available for feedback. Control is applied to these four state elements according to Equation 12. The time varying gain $K_1(t)$ that minimizes the cost function (9) is given by

$$K_1(t) = R^{-1}B_1^T S(t) \tag{13}$$

where S(t) is the solution of the associated matrix Riccati equation. An often used substitution for the optimal gain $K_1(t)$ is its constant steady state value $K_1 = K_1(\infty)$. The steady state value of S(t) is the solution of the algebraic Riccatti equation:

$$-\dot{S}(\infty) = S(\infty)A_1 + A_1^T S(\infty) - S(\infty) B_1 R^{-1} B_1^T S(\infty) + Q = 0 \tag{14}$$

The steady state gain solution is used in the simulations presented here.

7. Simulations With State Feedback

Figure 5 illustrates the simulated response of the design model (7) to a 4.8 inch step command, for various values of r. The simulations indicate that both the damped and undamped systems are capable of almost arbitrarily good performance as r is decreased. In practice, the limit on the response time is dictated by the strength of the beam and the torque limit of the actuator. A theoretical (assuming infinite beam strength and motor torque capacity) limit on the speed of response is discussed by Schmitz [6]. This limit is related to the non-minimum phase character of the tip position transfer function. Notice that the wrong way start phenomenon typical to systems with non-minimum zeros is indicated in the plots. Schmitz interprets the theoretical response limit as being roughly equivalent to a pure delay associated with the initial period during which the tip moves in the direction opposite to the control command.

When the state feedback law (12) is applied to the larger order systems (Figures 6 and 7), the excitation of the second mode of vibration is readily apparent when $r = 10^{-5}$. In the undamped system (Figures 6a and 7a) the oscillation takes more than two seconds to die out. Thus, in the case of the undamped system, we find that designing for higher performance (by reducing r) actually results in slower response. The excitation of the second mode also occurs in the damped system (Figure 6b and 7b), however, it dies out in about 0.8 seconds. Although the performance of the actual plant is not as good as that of the design model (Figure 5b), the simulation indicates that the response time for $r = 10^{-6}$ is slightly better than the lower levels of demanded performnce (larger values of r) considered. This is in sharp contrast with the results of Figures 6a and 7a for the undamped system. This example clearly indicates that the damped system is less susceptible to control spillover than the undamped case.

It should be noted that the peak control torque command, when $r = 10^{-6}$, is about 4800 inch pounds. This value is well above the beam's maximum bending moment capacity (~ 175 in. lbf. based on yield) and is about 60 times greater than the rated torque capacity (85 in.lbf.) of the experimental system's motor. In light of these figures, one might argue that control spillover is not a realistic concern for the system of interest. The author concedes to the somewhat artificial nature of this example, however, further consideration of the results adds to their significance. Suppose the initial step command is scaled down by a factor of 50 to about 0.1 inches. Because the system model is linear, we know that the corresponding peak torque is about 100 inch.lbf. This is a realistic figure for the system of interest. In Figures 6a and 7a, peak tip position oscillation amplitude is about 1.5 inches. Scaling this figure down by a factor of 50 gives 30 thousandths of an inch - a significant value in the context of robot accuracy.

8. Output Feedback

The simulations presented in the previous section were based on the assumed availability of states. Practical control systems must depend upon measured outputs for feedback. Frequently the outputs are different entities than the states. In contrast to systems using state feedback, output feedback systems are subject to instability as a consequence of model reduction [9-11] even when the neglected modes are asymptotically stable. This effect is sometimes called observation spillover.

In this section we follow the steady state LQR controller design approach employed in the previous section, however, we implement the controller using output feedback. The design model (A_1, B_1, C_1) has four states and four outputs and the measurement matrix C_1 is invertible. This allows us to calculate the state x_1 of the desing model from the output vector y according to:

$$x_1 = C_1^{-1} y \tag{15}$$

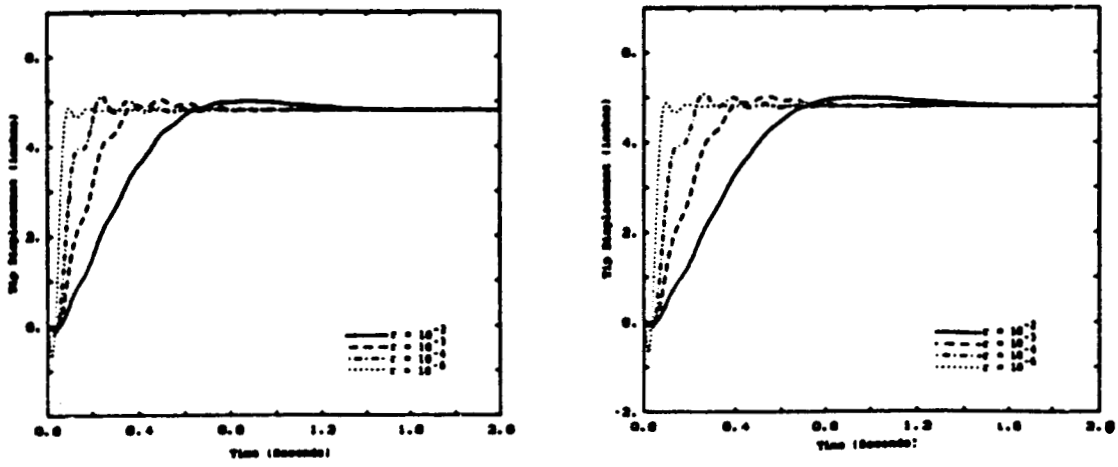

a) Undamped Case

b) Damped Case

Figure 5. Closed Loop Step Response Using State Feedback, One Vibration Mode Plant Model

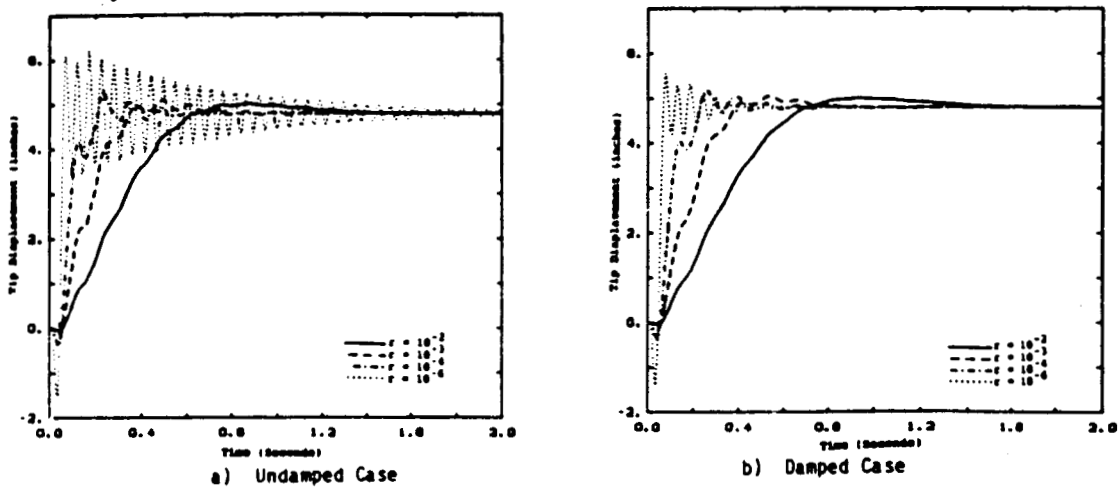

a) Undamped Case

b) Damped Case

Figure 6. Closed Loop Step Response Using State Feedback, Three Vibration Mode Plant Model

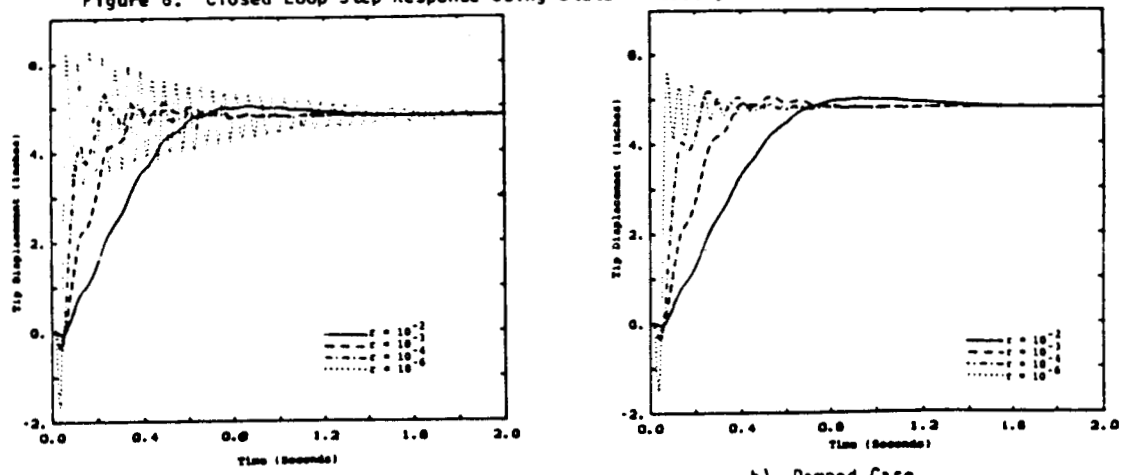

a) Undamped Case

b) Damped Case

Figure 7. Closed Loop Step Response Using State Feedback, Six Vibration Mode Plant Model

In this case the output feedback control law is given by:

$$u = -K_1 C_1^{-1} y \tag{16}$$

The output feedback law (16), when applied to the design model is equivalent to state feedback (12). When applied to controlling the actual model, the output feedback control law (16), expressed in the form of a state feedback law is given by:

$$u = -K_1 C_1^{-1} C_n x_n \tag{17}$$

Notice that when applied to the plant model, the output feedback law receives information from the states that were neglected in design. This is unwanted input (spillover), and can be viewed as a form of measurement corruption.

9. Simulations With Output Feedback

Simulation results obtained using output feedback are presented in Figures 8 through 10. Figures 8a and 8b are simulations of the design model using the output feedback law (16). When applied to the design model the output feedback law considered is equivalent to state feedback (Figure 5). This case is preseated here as a basis for comparison. When the low order output feedback law (16) is applied to the actual system models (Figure 9 and 10) we observe that the performance is limited by the onset of instability. In the undamped system, the first vibration mode is unstable for $r = 0.01$ and $r = 0.005$. The damped system remains stable under the same conditions, however, some first mode oscillatory behavior becomes evident as we attempt to design for higher performance. The damped system is not immune to tne instability experienced by the undamped case, however, due to its more favorable open loop pole placement it is more robust.

Upon comparison of the six mode and three mode systems, we find that the stable responses of the six mode plants do not differ noticeably from those of the three mode plants. On the other hand, the divergence rate of the unstable oscillations is greater in the six mode plant (Figure 10a) than in the three mode plant (Figure 9a). This indicates that the presence of the higher, neglected modes (4th, 5th and 6th) do affect system stability slightly.

This example illustrates that the passive damping treatment considered reduces the flexible system's susceptibility to observation spillover induced instability. The peak torque commanded at the highest performance (when the system is stable) was about 80 in.lbs., indicating that the performance demanded was reasonable for the system under consideration. The example employs perhaps the most simplistic of all possible output feedback schemes. Systems employing state estimators also rely on measured data for feedback, and they too are subject to instability due to modeling error.

10. Conclusion

One form of modeling error that is relevant for control of flexible structures results from ignoring high order vibration modes in the process of deriving a design model. The effects of this type of modeling error are manifested as control and observation spillover. We have presented simulations of multivariable control a particular flexible arm to illustrate that the addition of passive damping yields a system that is less susceptible to these undesirable effects.

To some degree these results follow intuition, in that one naturally expects that increasing the damping terms of a system's eigenvalues will provide a more stable system with improved performance. The results presented are intended to demonstrate the concept of passive damping on an example that is representative of practical lightweight manipulators.

11. Acknowledgements

The research described was performed at the Georgia Institute of Technology under the joint advisement of Dr. Wayne J. Book and Dr. Stephen L. Dickerson. The author was supported through a Research Assistantship provided by the Georgia Tech Material Handling Research Center (MHRC).

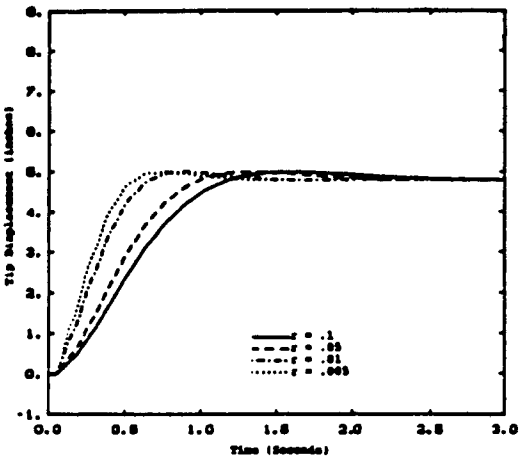

a) Undamped Case

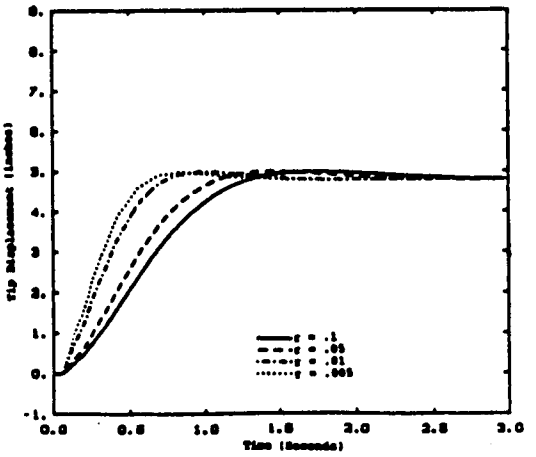

b) Damped Case

Figure 5. Closed Loop Step Response Using Output Feedback, One Vibration Mode Plant Model

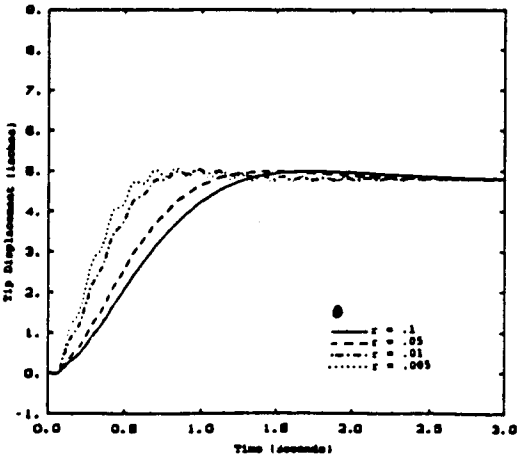

a) Undamped Case

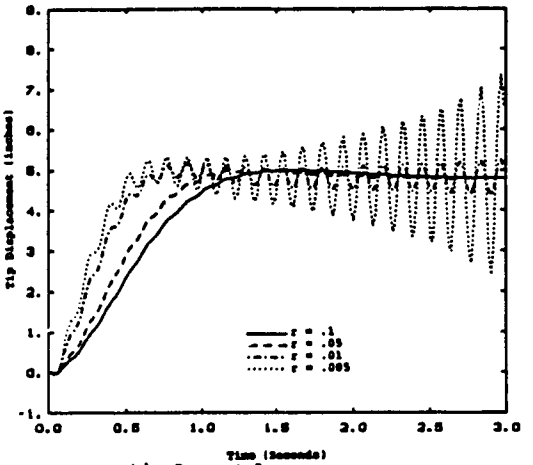

b) Damped Case

Figure 6. Closed Loop Step Response Using Output Feedback, ThreeVibration Mode Plant Model

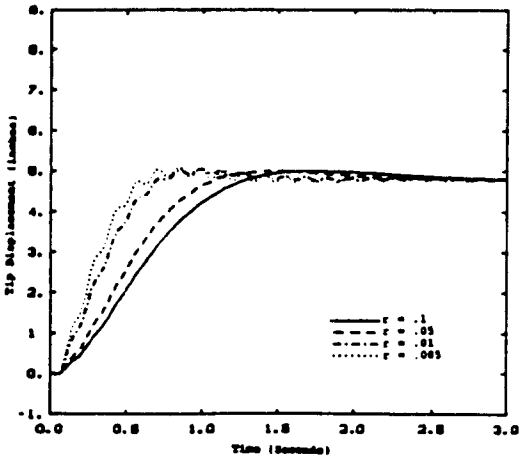

a) Undamped Case

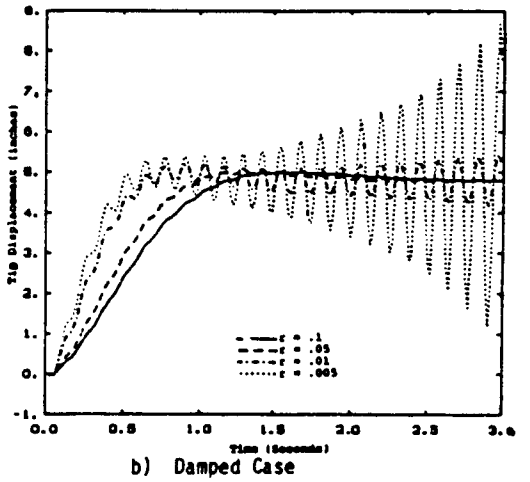

b) Damped Case

Figure 7. Closed Loop Step Response Using Output Feedback, Six Vibration Mode Plant Model

12. Bibliography

[1] Hastings, G.G., Controlling Flexible Manipulators, An Experimental Investigation, Ph.D. Dissertation, Dept. of Mech. Eng., Georgia Institute of Technology, August, 1986.

[2] Alberts, T.E., Augmenting the Control of a Flexible Manipulator with Passive Mechanical Damping, Ph.D. Dissertation, Ga. Tech., Sept. 1986.

[3] Alberts, T.E., Hastings, G.G., Book, W.J. and Dickerson, S.L., "Experiments in Optimal Control of a Flexible Arm with Passive Damping", Proc. 5th Symp. on Dynamics and Control of Large Structures, June 1985, pp. 423-435.

[4] Alberts, T.E., Book, W.J. and Dickerson, S.L., "On the Transfer Function Modeling of Flexible Structures with Distributed Damping", 1986 ASME Winter Annual Meeting, Dec. 1986.

[5] Plunkett, R. and Lee, C.T., "Length Optimization for Constrained Viscoelastic Layer Damping", J. Accoust. Soc. of Amer., Vol. 48, No. 1, 1970, pp. 150-16.

[6] Schmitz, E., "Experiments on the End-point Position Control of a Very Flexible One Link Manipulator", Ph.D Dissertation, Stanford Univ., Dept. of Aero & Astro., June 1985.

[7] Martin, G.D., On the Control of Flexible Mechanical Systems, Ph.D Dissertation, Stanford Univ., Dept. of E.E., May 1978.

[8] Breakwell, J.A., "Control of Flexible Spacecraft", Ph.D Dissertation, Stanford Univ., Dept. of Aero. & Astro., Aug. 1980.

[9] Balas, M.J., "Feedback Control of Flexible Systems", IEEE Trans. on Automatic Control, Vol. AC-23, No. 4, Aug. 1978, pp. 673-679.

[10] Blas, M.J., "Active Control of Flexible Systems", J. of Optim. Th. and App., Vol. 25, No. 3, July 1978, pp. 415-436.

[11] Khalil, H.K., "On the Robustness of Output Feedback Control Methods to Modeling Errors", IEEE Trans. on Automatic Control, Vol. AC-26, No. 2, April 1981.

APPENDIX A - System Parameters and Dimensions

Joint Inertia	J = 30.2 in^2.lbm.
Payload Mass	m = 0.09 lbm.
Joint Damping Coefficient	b = 0.10 in.lbf. s^2
Beam Dimensions	48" x 3/4" x 3/16"
Material	6065-T6 Aluminum

APPENDIX B - Transfer Function Poles and Zeros

Table B-1 Undamped System

Mode	System Poles		Hub Angle T.F. Zeros		Tip Position T.F. Zeros
1	-0.0541	±j7.726	-0.0149	±j2.1129	±8.3410
2	-0.1284	±j18.3456	-0.0985	±j14.0768	±45.0741
3	-0.2957	±j42.2446	-0.2853	±j40.7557	±111.3047
4	-0.5769	±j82.4188	-0.5719	±j81.6939	±206.9715
5	-0.9633	±j137.6207	-0.9603	±j137.1836	±332.0743
6	-1.4532	±j207.5965	-1.4511	±j207.2946	±486.6130

Table B-2 Damped System

Mode	System Poles		Hub Angle T.F. Poles		Tip Position T.F. Poles	
1	-.22197	±j7.1601	-.0176	±j1.9443	1 -7.2785,	+ 7.8830
2	-.9124	±j17.4515	-.6202	±j13.2581	2 -45.9556,	+44.7292
3	-2.3169	±j41.6716	-2.2342	±j40.1610	3 -97.7161,	+113.9306
4	-4.8477	±j83.2589	-4.7987	±j82.5101	4 -263.5548,	+216.0952
5	-8.5293	±j142.4761	-8.5042	±j142.0184	5 -389.2245,	+351.1999
6	-11.7674	±j219.5993	-11.7581	±j219.2929	6 -554.2140,	+519.0317